

## On-chip optical tweezers based on freeform optics: supplement

**SHAOLIANG YU,<sup>1,†,\*</sup>  JINSHENG LU,<sup>2,3,†</sup>  VINCENT GINIS,<sup>2,4</sup>   
SIMON KHEIFETS,<sup>2</sup> SOON WEI DANIEL LIM,<sup>2</sup>  MIN QIU,<sup>5</sup> TIAN  
GU,<sup>6</sup> JUEJUN HU,<sup>1,6,7</sup> AND FEDERICO CAPASSO<sup>2,8</sup>**

<sup>1</sup>*Department of Materials Science and Engineering, Massachusetts Institute of Technology, Cambridge, Massachusetts 02139, USA*

<sup>2</sup>*Harvard John A. Paulson School of Engineering and Applied Sciences, Harvard University, Cambridge, Massachusetts 02138, USA*

<sup>3</sup>*State Key Laboratory of Modern Optical Instrumentation, College of Optical Science and Engineering, Zhejiang University, Hangzhou, 310027, China*

<sup>4</sup>*Data Lab/Applied Physics, Vrije Universiteit Brussel, 1050 Brussels, Belgium*

<sup>5</sup>*Key Laboratory of 3D Micro/Nano Fabrication and Characterization of Zhejiang Province, School of Engineering, Westlake University, Hangzhou, 310024, China*

<sup>6</sup>*Materials Research Laboratory, Massachusetts Institute of Technology, Cambridge, Massachusetts 02139, USA*

<sup>7</sup>*e-mail: [hujuejun@mit.edu](mailto:hujuejun@mit.edu)*

<sup>8</sup>*e-mail: [capasso@seas.harvard.edu](mailto:capasso@seas.harvard.edu)*

*\*Corresponding author: [yusl@mit.edu](mailto:yusl@mit.edu)*

*†These authors contributed equally to this paper.*

---

This supplement published with The Optical Society on 12 March 2021 by The Authors under the terms of the [Creative Commons Attribution 4.0 License](https://creativecommons.org/licenses/by/4.0/) in the format provided by the authors and unedited. Further distribution of this work must maintain attribution to the author(s) and the published article's title, journal citation, and DOI.

Supplement DOI: <https://doi.org/10.6084/m9.figshare.14077373>

Parent Article DOI: <https://doi.org/10.1364/OPTICA.418837>

# On-chip optical tweezers based on freeform optics: supplemental document

## 1. Fabrication process flow

**Waveguide fabrication (Fig. S4a).** We first patterned metal marks on a silicon wafer to facilitate alignment between the waveguide and the freeform optics. A 10- $\mu\text{m}$  layer of OrmoCore was then spin-coated on the silicon substrate as a bottom cladding layer, cured by a UV lamp under nitrogen atmosphere, and baked at 130 °C for 10 min. A 2.5- $\mu\text{m}$  layer of EpoCore was subsequently spin-coated on top of the bottom cladding layer as the waveguide core, followed by a soft bake at 90 °C for 2 min. The waveguides were defined using an i-line UV stepper (AutoStep 200, GCA) with a dose of 150 mJ/cm<sup>2</sup>, baked at 90 °C for 5 min, and developed in SU-8 developer for 1 min. After 10 s surface activation in O<sub>2</sub> plasma, another 10- $\mu\text{m}$  layer of OrmoCore was added on top of the waveguide as a top cladding layer following the same procedures of forming the bottom cladding layer.

**Deep trench etching (Fig. S4b).** A Cr/Cu (5/200 nm) metal mask was patterned on top of the waveguide structures through a lift-off process. The pattern was transferred into the waveguide layer stack to form deep trenches via reactive ion etching (RIE, PlasmaPro 100 Cobra, Oxford Instruments). CF<sub>4</sub> and O<sub>2</sub> were used as etching gases with flow rates of 30 and 20 sccm, respectively. The inductively coupled plasma (ICP) and RF power loads were set to 1500 W and 75 W, respectively. The etch rate is approximately 500 nm/min at 20 °C.

**Freeform optics fabrication (Fig. S4c).** A 20- $\mu\text{m}$  layer of EpoCore was spin-coated on top of the waveguide stack to completely fill the deep trench, followed by a soft bake of 10 min at 90 °C. The sample was then mounted on the 3-D printing station (Photonic Professional GT, Nanoscribe GmbH) for two photon polymerization in a dip-in laser lithography (DiLL) mode. A 63x lens was used for writing with an index matching oil ( $n = 1.598$ ) filling the gap between the lens and the sample. The silicon substrate/bottom cladding interface was used as a datum plane to locate the height of the waveguide. Along the lateral direction, the freeform optics were aligned to the pre-defined metal marks on the substrate. The 3-D structures were exposed with 17.5-mW (100 fs, 80 MHz, 780 nm) laser power at a speed of 5 mm/s, with slicing and hatching distance set to be 200 nm and 100 nm, respectively. The sample was baked at 90 °C for 10 min before development in SU-8 developer for 5 min.

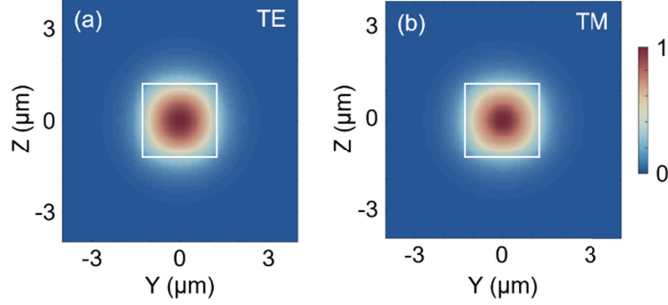


Fig. S1. Mode profile of the fundamental (a) Transverse Electric (TE) mode and (b) Transverse Magnetic (TM) mode of the waveguide.

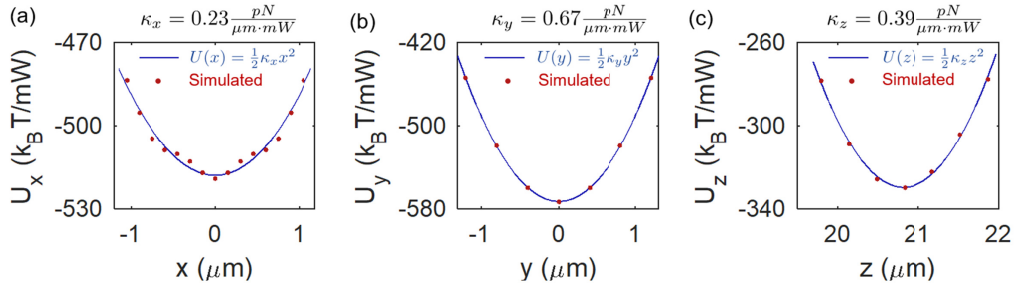


Fig.S2. Simulated trapping stiffness of the focusing reflector-based optical tweezers. Trapping stiffness is obtained by fitting the simulated trapping potential data with a harmonic well.

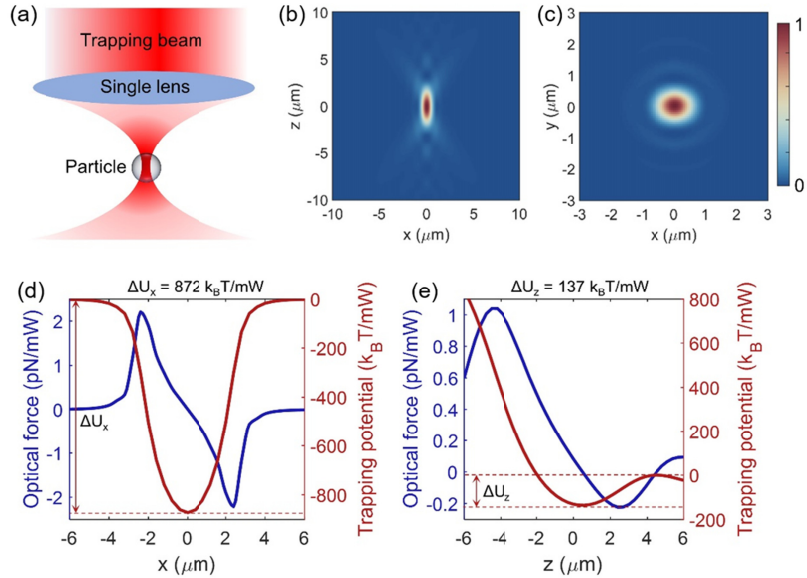


Fig. S3. Optical trapping with a single Gaussian beam. (a) Illustration diagram of the particle trapped by a Gaussian beam with NA=1.0. Simulated beam profile on the (b) longitudinal and (c) transverse planes at the focal spot. Calculated optical forces (blue line) and trapping potentials (red line) along the (d) transverse and (e) longitudinal directions, with a trapping potential depth of 872 kBT/mW and 137 kBT/mW, respectively. The index and particle size are set to be the same as the experimental parameters.

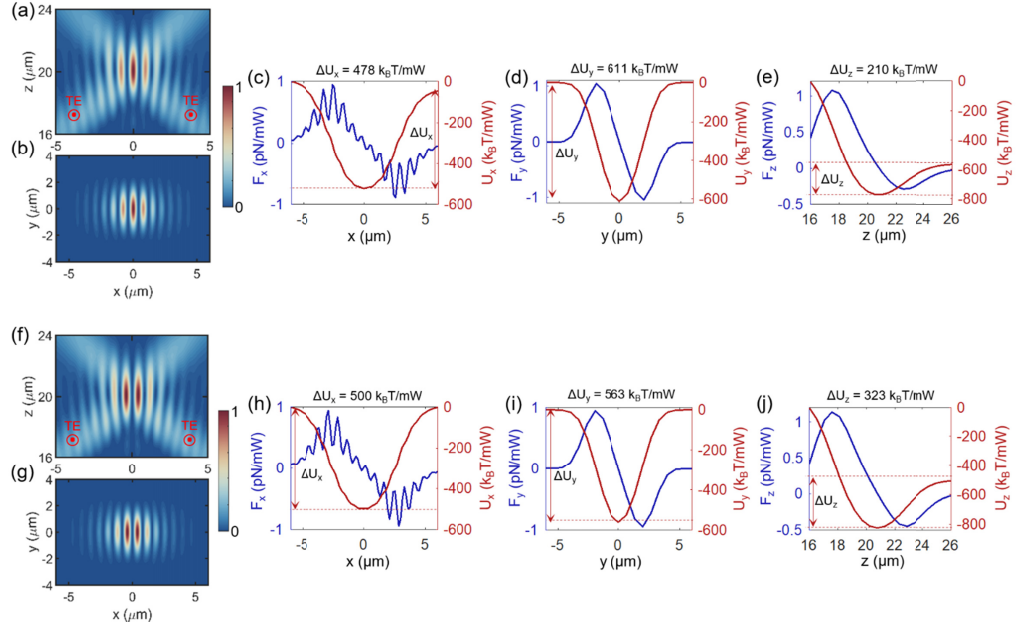


Fig. S4. Numerical simulations of optical forces and trapping potentials for the focusing reflector-based optical tweezers when there are phase and power variations between the two beams. (a-e) Simulated intensity distribution on the XZ (a) and XY (b) planes at the focal spot and optical forces and trapping potentials along X-, Y-, and Z-directions when the power from the right-side waveguide is 10% less than that of the left-side waveguide. (f-j) Simulated intensity distribution on the XZ (f) and XY (g) planes at the focal spot and optical forces and trapping potentials along X-, Y-, and Z-directions when the two beams have a  $\pi$  phase difference.

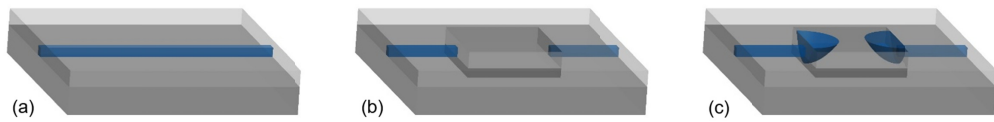


Fig. S5. Fabrication flow of the on-chip optical tweezer. (a) Patterning the waveguides via UV photolithography. (b) Etching the deep trench by reactive-ion etching. (c) Sculpting the free-from micro-optics using two-photon polymerization.

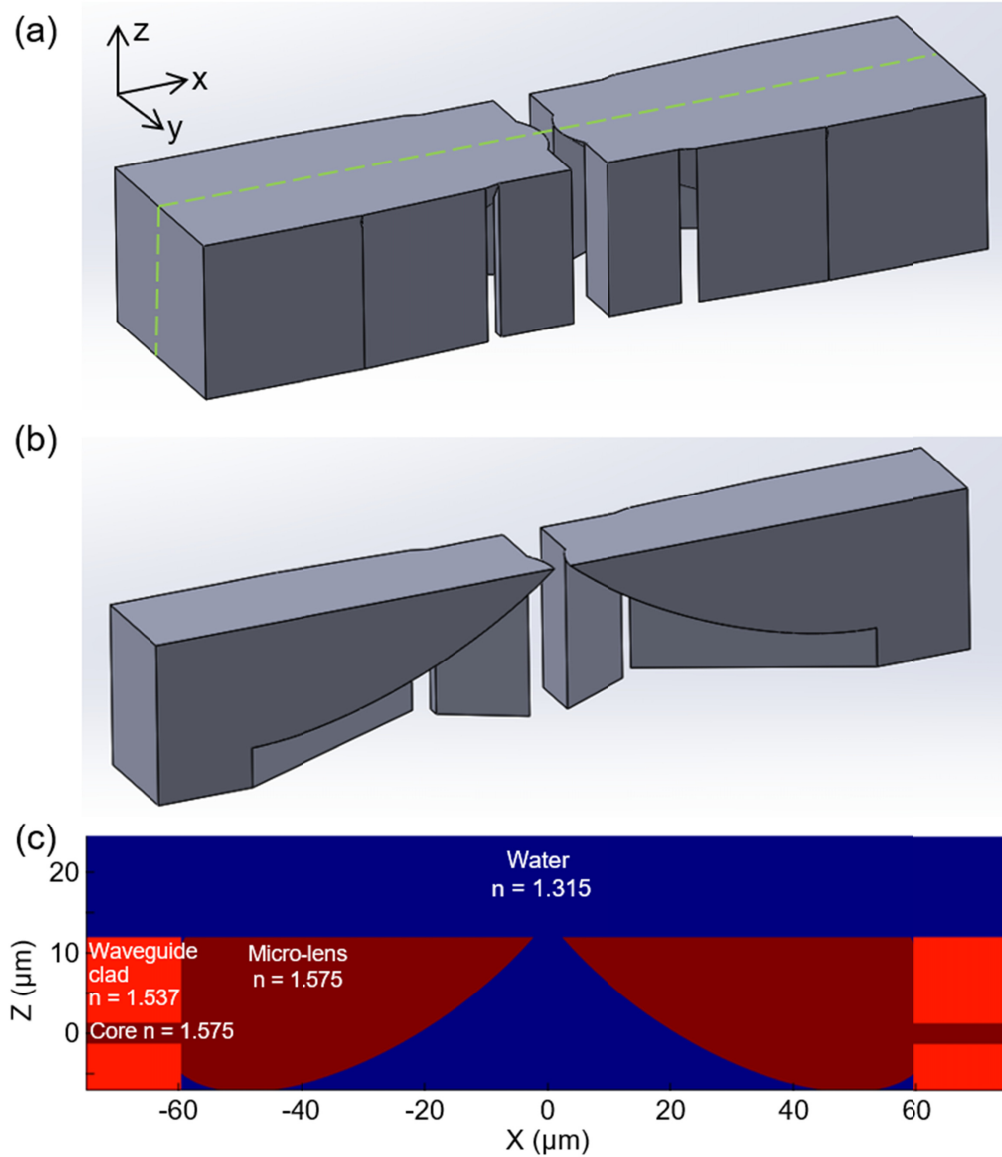


Fig. S6. Geometry of the focusing reflectors. (a) Sideview and (b) section view along the green line of (a) of the 3D structures for writing the free-form reflectors. There are additional structures connected to the 3D micro-optics to provide mechanical support. (c) Refractive index distribution along the cross section of the focusing reflectors.

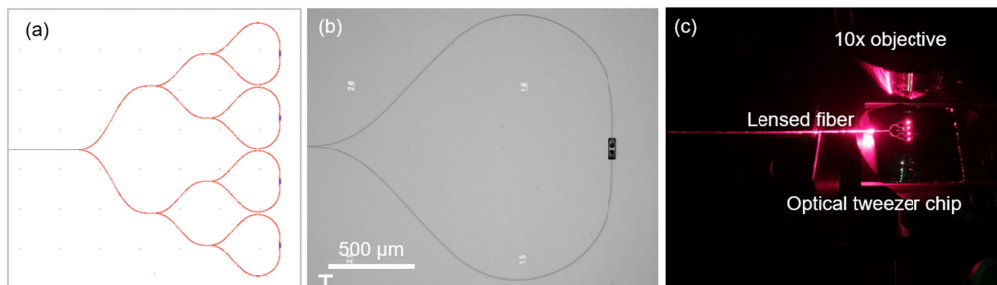


Fig. S7. Images of the device. (a) Layout design of the device array. (b) Optical microscope images of the fabricated Y-branch waveguide. (c) Photograph of the device when a 660-nm wavelength laser is coupled into the waveguide via a lensed fiber.

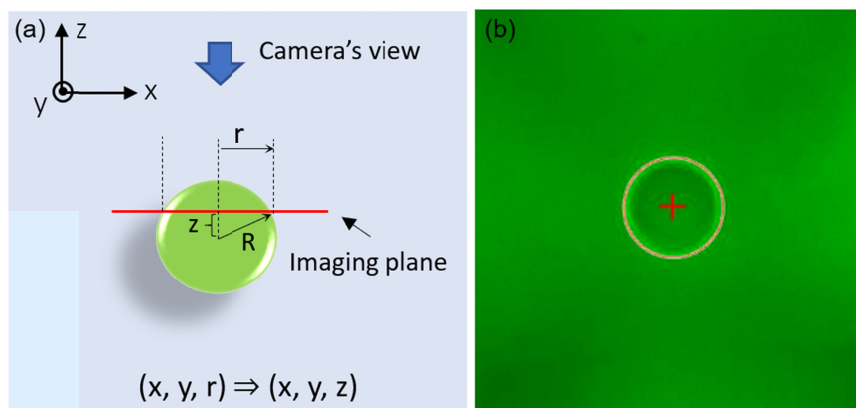


Fig. S8. Extraction of the position of the trapped particle. (a) The vertical position  $z$  was calculated by comparing the particle diameter  $R$  with the captured diameter  $r$ ,  $z = \sqrt{R^2 - r^2}$ . (b) Optical microscope image of the trapped particle. Here a circular Hough transform algorithm is used to find the  $x$  and  $y$  position and the captured diameter ( $r$ ) of the particle.

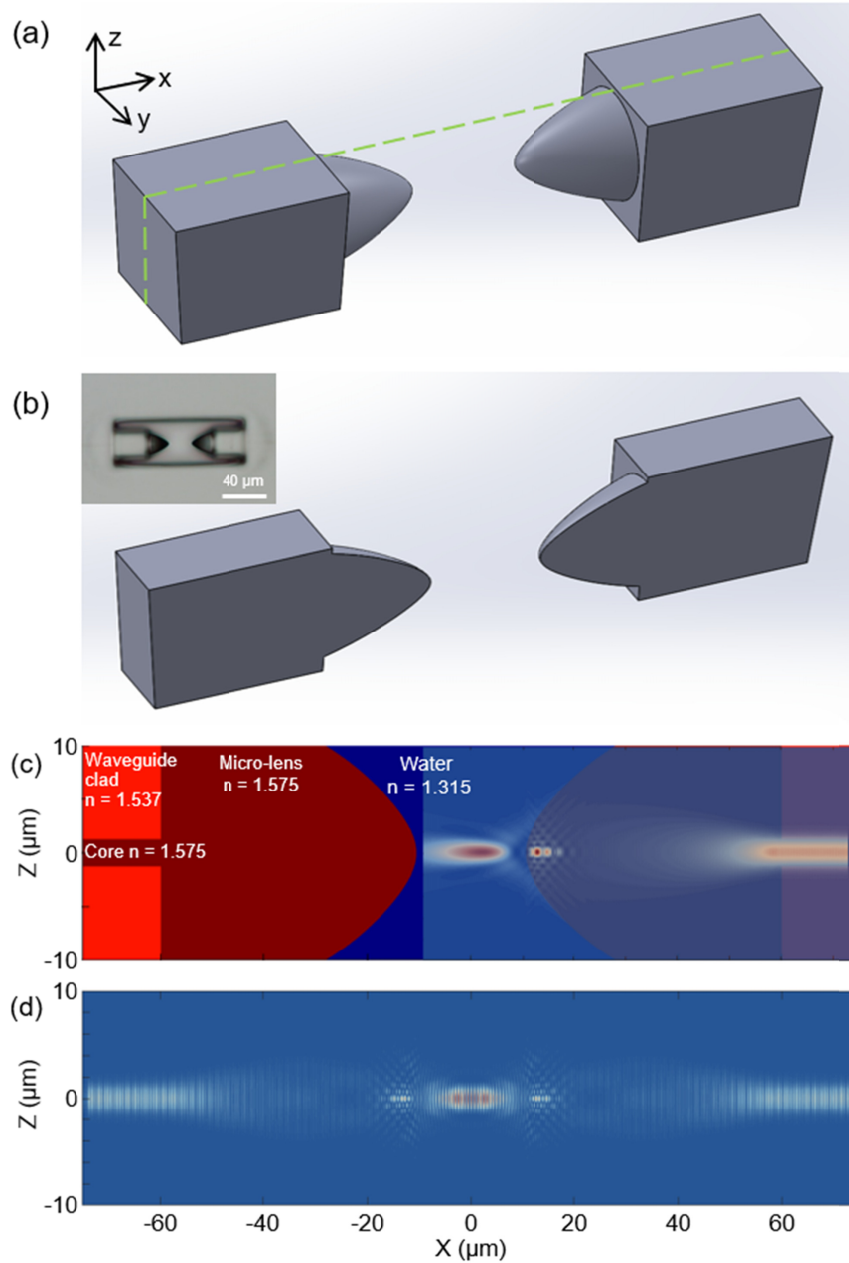


Fig. S9. Geometry of the refractive micro-lenses. (a) Sideview and (b) section view along the green line of (a) of the 3D structures for writing the free-form micro-lenses. Extra features are added to the lens for mechanical supporting. Inset of (b) is a top-view optical microscope image of the fabricated device. (c) Refractive index distribution along the cross section of the micro-lenses, with the right side overlapped to the beam profile focused by a single micro-lens. (d) Intensity distribution of two counter-propagating beams focused by the two micro-lenses.

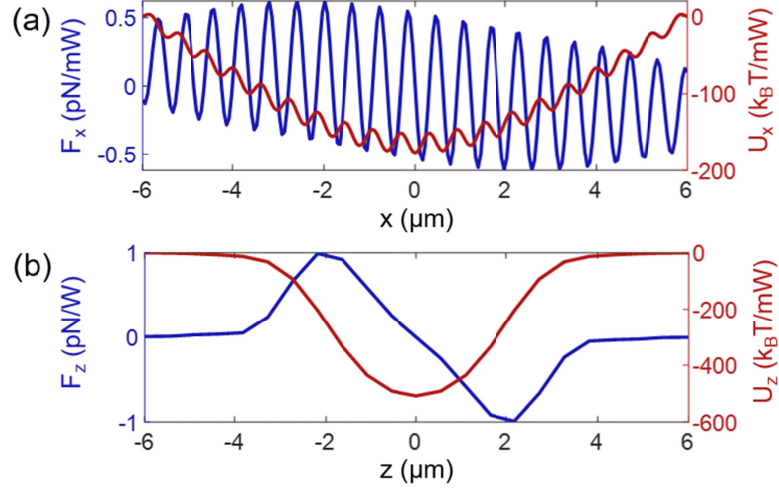


Fig. S10. Simulated optical force and trapping potential of the refractive micro-lens based tweezer for a single particle. The optical force (blue line) and trapping potential (red line) in the (a) longitudinal and (b) transverse direction.

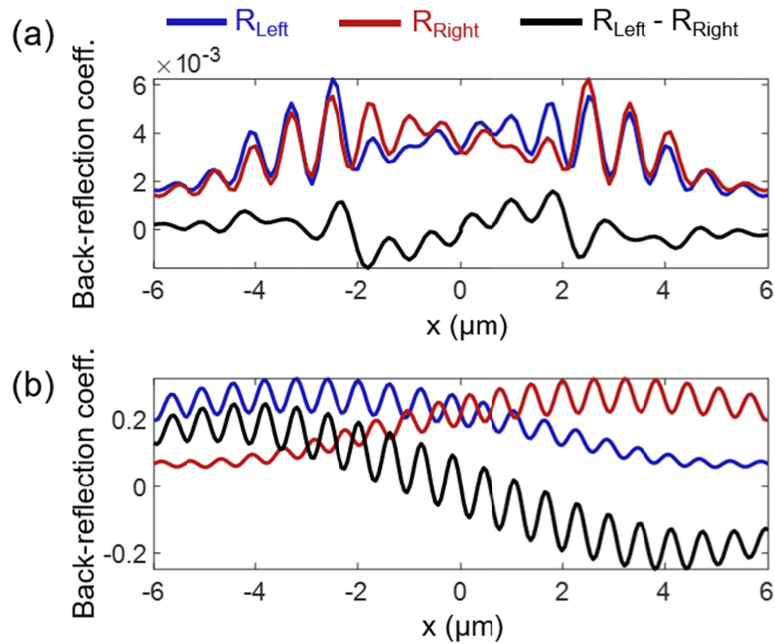


Fig. S11. Simulated reflected power back into the waveguide ports of the (a) focusing reflector and (b) refractive micro-lens based tweezer for a single particle as a function of the displacement along the longitudinal direction. The blue lines, red lines, and black lines are the reflectance in the left port, the reflectance in the right port, and the reflectance difference between the two ports, respectively.